Proc. of the 9th Intl. Conf. of Asian Society for Precision Engg. and Nanotechnology (ASPEN 2022)
15–18 November 2022, Singapore. Edited by Nai Mui Ling Sharon and A. Senthil Kumar
doi://10.3850/978-981-18-6021-8_OR-07-0157

Parametric model and optimization conditions in high-frequency ultrasonic vibration-assisted turning of optical spherical convex mold

Xiaoliang Liang[1,2], Canbin Zhang[1,2], Chunjin Wang[1], Chi Fai Cheung[1,#]

1 State Key Laboratory of Ultra-Precision Machining Technology, Department of Industrial and Systems Engineering, The Hong Kong Polytechnic University, Kowloon, Hong Kong, China)
2 These authors contributed equally to this work.
Corresponding Author / Email: benny.cheung@polyu.edu.hk, TEL: +852-64726812, FAX: +852-64726812
KEYWORDS: Ultrasonic-assisted vibration turning; Convex mold; Parametric model; Parameter optimization; Ultra-precision machining

Ultrasonic vibration-assisted cutting improves the machinability of difficult-to-cut materials to achieve nanoscale superfinished surfaces. This work focused on the parametric model and optimization conditions in high-frequency ultrasonic vibration-assisted turning of optical spherical convex mold, including tool radius r, cutting speed v, feed rate f, vibration amplitude A, slope angle S. Firstly, the parametric model for predicting surface roughness based on response surface method (RSM) was established. The adequacy of parametric model was proved by analysis of variance. Secondly, the effects of cutting conditions and their interaction on surface roughness were analyzed. Experimental results indicated that the influence degrees of cutting conditions on surface roughness were inconsistent, which the percentage contribution of r, v, f, A, and S to the surface roughness were 14.44%, 3.51%, 34.41%, 2.64% and 27.75%, respectively. Higher tool radius and vibration amplitude decrease surface roughness while the elevated of cutting speed, feed rate and slope angle increased the surface roughness. Based the parameter optimization as the solution of desirability function, the most ideal cutting conditions with the desirability value of 0.717 was r=1 mm, v=2.99 m/min, f=6.7 μm/rev, A=2.4μm, S=0-15° achieved the goals of surface roughness and material removal rate.

1. Introduction

Diamond turning belongs to an ultra-precision machining technique that produces precision components with assured form accuracy and surface roughness in the nano-scale range. In order to reduce tool wear, several researchers have been developed in ultrasonic vibration-assisted machining, which was considered as a promising technology enabling superior cutting performance including lower cutting forces, better surface finish, higher cutting stability and longer tool life [1,2].

Surface roughness was closely related to cutting parameters, tool geometry and ultrasonic vibration parameters. Zhang et al. [3] carried out the elliptical ultrasonic vibration-assisted face-turning experiments on hardened steels by using diamond tools at various nominal cutting speeds, depth of cut, and feed rate, indicating that surface roughness increased with the increase of cutting speed and feed rate. The mirror-like surface roughness of 10 nm was also achieved under the optimal combination of cutting parameters. Klocke et al. [4] investigated the effect of vibration frequency of 40 kHz and 60 kHz on surface roughness during turning steel, indicating that the elevated frequency reduced surface roughness. They also considered that the increase in frequency led to a stable cutting process since the same contact ratio between the tool and workpiece during cutting required smaller amplitudes.

If the cutting conditions are not properly selected, the process can lead to violations of machine constraints or reduced productivity. The response surface method (RSM) is a statistical and mathematically based analysis technique that can be used for development, improvement, and optimization efforts. Several studies used the RSM to investigate the cutting factors (cutting speed, feed rate, and depth of cut) on surface roughness and tool wear [5, 6]. The established mathematical model predicted the response within the range, among which the best optimization process was obtained.

In this work, the parametric model and optimization conditions in high-frequency ultrasonic vibration-assisted turning optical spherical convex mold were studied based on RSM. The effects of cutting conditions and their interaction on surface roughness were analyzed. Based the parameter optimization as the solution of desirability function, the most ideal cutting conditions were achieved.

2. Experimental setup

As shown in Fig. 1, the turning experiments were performed on an ultra-precision machine tool Nanotech 450. The high-frequency ultrasonic vibration-assisted system (Son-X UTS2) was used to assist the turning process with the vibration frequency of 104 kHz. During the turning process, the cutting tool was equipped with vibrations that moved parallel to the cutting direction. The constant surface velocity

mode was used, which the spindle speed increased steadily as the tool moved inwards different regions of the sphere of different diameters. Since the changes in the cutting position of tool edge, the geometry of spherical convex mold affected the surface roughness.

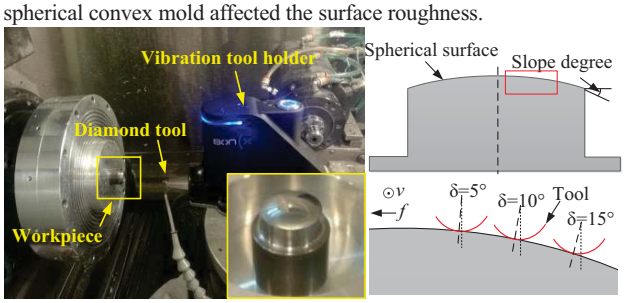

Fig. 1 Experimental setup for high-frequency ultrasonic vibration-assisted cutting system

3. Experimental design

The tool radius r (mm), cutting speed v (m/min), feed rate f (μm/rev), vibration amplitude A (μm), slope angle S (°) were experimental variables. Three levels were chosen for each factor to cover research interests. The response variables were surface roughness Sa (nm) and material removal rate (mm^3/min). As shown in Eq. (1), the final model consisted of purely numerical term, linear term, two interaction terms, and second-order term. The I-optimal criterion was used to determine the effects of cutting conditions on surface roughness. As shown in Table 1, the experimental factors and response variables were listed.

$$Y = \beta_0 + \sum_{i=1}^{k} \beta_i x_i + \sum_{i=1}^{k} \sum_{j=1}^{k} \beta_{ij} x_i x_j + \sum_{i=1}^{k} \beta_{ii} x_{ii}^2 \qquad (1)$$

where Y was the response variables. i and j refered to numeric factors. x_i was the input experimental factors. β_0 was the fixed numerical term. β_i, β_{ij}, and β_{ii} were the coefficients of linear, quadratic, and cross product terms, respectively.

Table 1 Experimental factors and response variables

Run	Factors					Responses	
	r	*v*	*f*	*A*	*S*	*MMR*	*Sa*
1	1	2	10	2.4	15	0.1	7.1
2	1	4	2.5	2.4	5	0.05	4.7
3	0.3	4	2.5	2.4	15	0.05	9.7
4	1	4	5	2.4	15	0.1	11.5
5	0.5	4	5	1.8	10	0.1	7.8
6	0.5	3	5	2.4	10	0.075	6.1
7	1	4	10	2.4	5	0.2	8.2
8	0.3	3	10	1.8	10	0.15	10.9
9	0.3	4	5	2.4	5	0.1	6.5
10	0.3	3	5	1.8	15	0.075	12.5
11	0.3	3	10	1.8	10	0.15	11.1
12	0.5	3	2.5	1.2	10	0.0375	7.9
13	1	3	5	1.2	5	0.075	4.6
14	1	2	2.5	2.4	15	0.025	5.9
15	1	4	10	1.2	10	0.2	8.2
16	0.5	2	10	1.8	15	0.1	13.3
17	0.5	2	2.5	1.8	5	0.025	4.2
18	0.3	2	10	2.4	5	0.1	9.7
19	0.5	4	10	2.4	10	0.2	9.2
20	0.3	4	2.5	1.2	15	0.05	13.2
21	0.5	4	5	1.8	10	0.1	7.9
22	0.5	3	5	2.4	10	0.075	6.3
23	0.3	2	5	1.2	15	0.05	10.2
24	0.5	3	10	1.8	5	0.15	9.4
25	0.5	3	10	1.8	5	0.15	9.7
26	0.5	4	10	1.2	15	0.2	14.2
27	0.5	2	10	1.2	10	0.1	12.4
28	0.3	4	2.5	1.2	5	0.05	5.2
29	0.3	2	2.5	2.4	15	0.025	8.6
30	0.5	4	5	1.8	10	0.1	7.9
31	1	3	2.5	1.2	15	0.0375	6.3

4. Results and discussions

4.1 Quantitative analysis of data

The analysis of variance (ANOVA) implied the importance of design parameters to survey response parameters. The ANOVA for parametric model was listed as shown in Table 2. The significance of each coefficient was evaluated by the p-value, which the p-value less than 0.05 meant important factor while the terms were not significant with the value greater than 0.1. As a result, r, v, f, A, S were all significant factors, and the percentage contribution to surface roughness were 14.44%, 3.51%, 34.41%, 2.64% and 27.75%, respectively. The lack of fit indicated that the value of 152.67 was significant in relation to the pure error, which indicated the initial model need to be revised to better fit.

Table 2 ANOVA of parametric model for experimental factors

Source	*Sum of squares*	df	*Mean square*	F-values	p-values	Contrib.
Model	212.19	20	10.61	7.53	0.0012	
r	24.05	1	24.05	17.07	0.0020	14.44%
v	5.84	1	5.84	4.15	0.0691	3.51%
f	57.31	1	57.31	40.68	<0.0001	34.41%
A	4.39	1	4.39	3.12	0.1079	2.64%
S	46.22	1	46.22	32.81	0.0002	27.75%
*r*v*	3.57	1	3.57	2.54	0.1424	2.14%
*r*f*	1.09	1	1.09	0.7765	0.3989	0.65%
*r*A*	6.45	1	6.45	4.58	0.0580	3.87%
*r*S*	0.8787	1	0.8787	0.6238	0.4480	0.53%
*v*f*	2.92	1	2.92	2.07	0.1807	1.75%
*v*A*	0.1309	1	0.1309	0.0930	0.7667	0.079%
*v*S*	3.23	1	3.23	2.29	0.1611	1.94%
*f*A*	0.9892	1	0.9892	0.7022	0.4216	0.59%
*f*S*	3.57	1	3.57	2.53	0.1426	2.14%
*A*S*	0.0458	1	0.0458	0.0325	0.8605	0.03%
r^2	0.3619	1	0.3619	0.2569	0.6232	0.22%
v^2	0.0031	1	0.0031	0.0022	0.9636	0.01%
f^2	0.0412	1	0.0412	0.0293	0.8676	0.02%
A^2	0.0081	1	0.0081	0.0058	0.9410	0.01%
S^2	5.47	1	5.47	3.88	0.0772	3.28%
Residual	14.09	10	1.41			
lack of fit	13.99	5	2.80	152.67	<0.0001	
Pure error	0.0917	5	0.0183			

As a result, the non-significant lack of fit was beneficial in

ensuring the appropriate parametric model. The final regression equation for significant experimental factors and response variables was shown in Eq. (2).

$$Sa = 12.702 - 18.164r - 1.176v + 1.606f - 2.163A - 0.598S + 2.287r*v + 3.847r*A - 0.135v*f + 0.128v*S - 0.203f*A - 0.031f*S + 0.039S^2 \quad (2)$$

As shown in Table 3, the analysis of fit statistics was performed on the final regression equation. The p-values were all calculated less than 0.0001. The determination coefficient (R^2) was 0.9244, indicating that the proposed model had good response variability. The differences between Adjusted R^2 and Predicted R^2 were all less than 0.17 indicating that the model was reasonably consistent. As shown in Fig. 2, the comparative analysis between experiment and prediction was presented. All experimental values were distributed around the prediction regression, indicating that the error of prediction was acceptable.

Table 3 Fit statistics for finial parametric model

Std. Dev.	R^2	Adj. R^2	Pre. R^2	Adeq. Pre.
0.9749	0.9244	0.8740	0.7036	16.59

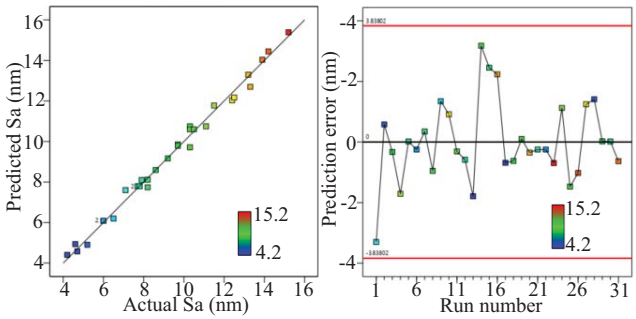

Fig. 2 Comparative analysis between experiment and prediction.

4.2 Effects of cutting conditions on surface roughness

Fig. 3 showed the perturbation map of various experimental factors and the surface response profiles of interacting factors. With the increase of the tool nose radius, surface roughness presented a nonlinear decreasing trend. This was mainly related to the theoretical residual height reduction of the machined surface as the tool nose radius increased [7]. Conversely, surface roughness showed a linear increase trend since the increase of the feed rate improved the residual height. Moreover, surface roughness showed a slight upward trend with the increase of cutting speed. The enhanced cutting speed contributed mostly to such result by increasing the ratio between cutting speed and maximum vibration speed. In addition, the increase of cutting speed also resulted in more material being removed per vibration cycle, reducing the overlap of cutting paths. With the increase of vibration amplitude, surface roughness showed a downward trend. The reduction in duty cycle could enhance lubrication and cooling conditions, improving cutting stability and surface finish. The increase of slope angle led to the deterioration of surface quality, and surface roughness showed a sharp increase trend. The vibration amplitude was changed along the tool edge, which the tool tip vibrated with the maximum amplitude and the amplitude gradually decreased from the nose center to the side. The tool tip was used to machine the geometries of low slope angle while the side parts were used to machine geometries of high slope angle. As a result, the lubrication and heat transfer were better for machining conditions at the positions of low slope angle, which reduced the surface roughness. Furthermore, the clear interactions were presented between cutting conditions based on surface response profiles of the interacting factors. Surface roughness could be further minimized by raising the tool radius and vibration amplitude while decreasing the cutting speed, feed, and slope angle.

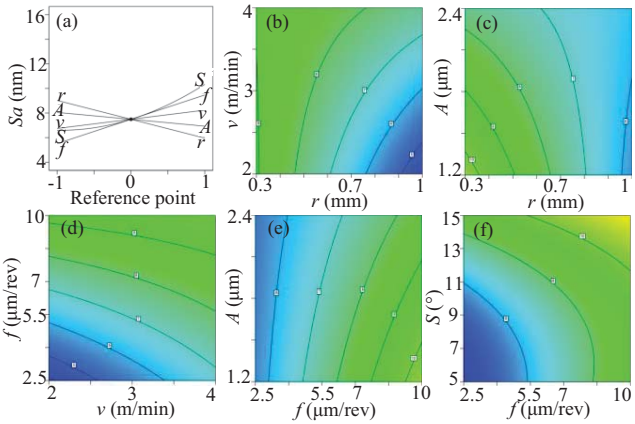

Fig. 3 Perturbation map of various experimental factors and the surface response profiles of interacting factors.

4.3 Desirability optimization and confirmation test

As shown in Eq. (3), the desirability function was used to realize the optimization analysis. Based on actual requirements, the specific target settings were shown in Table 4. The required surface roughness of all workpiece should be less than 10 nm. The numerical optimization was performed by using Design Expert software to find the factor settings that satisfied the defined goals.

$$D = (d_1^{r_1} \times d_2^{r_2} \times \ldots d_i^{r_i})^{\frac{1}{\sum r_i}} = \left(\prod_{i=1}^{n} d_i^{r_i}\right)^{\frac{1}{\sum r_i}} \quad (3)$$

Where D was desirability function value. d_i was the desirability parameter for factors and variables. n was the parameter number. The significance of the parameter was denoted by r_i. The optimization weights were set equal for all parameters. The desirability function value varied from 0 to 1, in which closer to 1 denoting more desire.

Table 4 Limitations and objectives for cutting conditions optimization.

Factors and responses	Goal	Lower	Upper	Weight
r (mm)	Minimize	0.3	1	1
v (m/min)	Minimize	2	4	1
f (μm/rev)	Maximize	2.5	10	1
A (μm)	In range	1.2	2.4	1
S (°)	In range	5	15	1
MMR	In range	0.1	0.2	1
Sa (nm)	In range	5	15	1

Fig. 4 displayed the desirability function graphs for each experimental factor and interactive factors. It was noted that the desirability function value of all factors satisfied the limitations and objectives for cutting conditions optimization. The desirability function values of the experimental factors and interactive factors have matched the maximum value of 0.717. According to the result of

desirability function optimization, the most ideal cutting conditions were r=1 mm, v=2.99 m/min, f=6.7 μm/rev, A=2.4 μm, S=0-15°. As shown in Fig. 5, the comparative analysis of experimental and predicted results under the optimal criterion was displayed. Such result showed that the predicted values matched the experimental values quite well. As shown in Fig. 6, the surface topography in different regions of the convex spherical mold was presented. The corresponding surface roughness of the inclination 5°, 10°, 15° were 4.801 nm, 6.625 nm, and 9.205 nm, respectively.

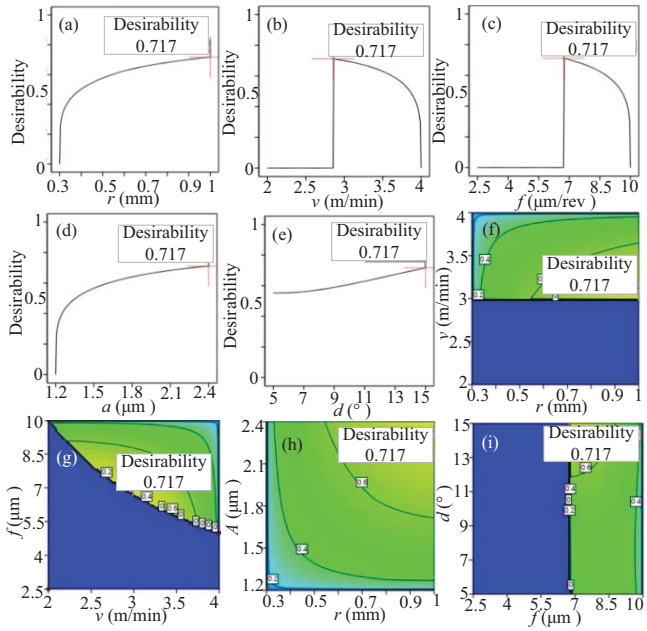

Fig. 4 Desirability function graphs for each experimental factor and interactive

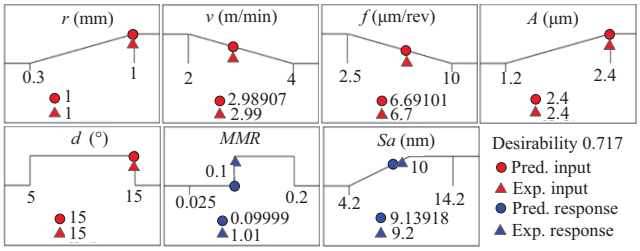

Fig. 5 Optimization solution and validation for experimental factors and response variables.

5. Conclusions

The parametric model for predicting surface roughness based on RSM was established. The adequacy of prediction model was proved by analysis of variance. The percentage contribution of r, v, f, A, S to surface roughness were 14.44%, 3.51%, 34.41%, 2.64% and 27.75%, respectively. The clear interactions were presented between cutting conditions. Higher tool radius and vibration amplitude decrease surface roughness while the elevated of cutting speed, feed rate and slope angle increased the surface roughness. The optimization conditions with the desirability value of 0.717 was r=1 mm, v=2.99 m/min, f=6.7 μm/rev, A=2.4 μm, S=0-15°. The predicted values matched the experimental values quite well.

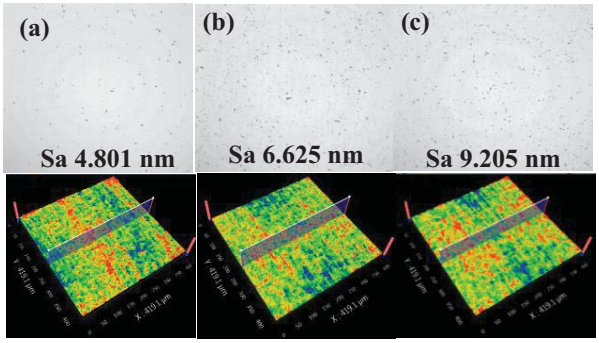

Fig. **6** Surface topography of the convex spherical mold for confirmation test, (a) 5°, (b) 10°, (c) 15°.

ACKNOWLEDGEMENT

The authors would like to express their sincere thanks for the financial support from the Research Office (project code: RK2Z) from The Hong Kong Polytechnic University. Special thanks are also due to the contract research project between the State Key Laboratory of Ultra-precision Machining Technology of The Hong Kong Polytechnic University and Son-X, Gmbh, Aachen, Germany.

REFERENCES

1. Gaidys, R., Dambon, O., Ostasevicius, V., et al., "Ultrasonic tooling system design and development for single point diamond turning (SPDT) of ferrous metals," Int. J. Adv. Manuf. Tech., Vol. 93, No. 5, pp. 2841-2854, 2017.
2. Arefin, S., Zhang, X.Q., Anantharajan, S.K., et al, "An analytical model for determining the shear angle in 1D vibration-assisted micro machining," Nanomanuf. Metrol., Vol. 2, No. 4, pp. 199-214, 2019.
3. Zhang, X., Kumar, A.S., Rahman, M., et al., "Experimental study on ultrasonic elliptical vibration cutting of hardened steel using PCD tools," J. Mater. Process. Tech., Vol. 211, No. 11, pp. 1701-1709, 2011.
4. Klocke, F., Dambon, O., Bulla B., "Ultrasonic assisted diamond turning of hardened steel with mono-crystalline diamond," Proceedings of the 10th International Euspen Conference, pp. 165-169, 2008.
5. Liu. Y., Zhou, J., Fu, W., et al., "Study on the effect of cutting parameters on bamboo surface quality using response surface methodology," Measurement, Vol. 174, pp. 109002, 2021.
6. Li, X., Liu, Z., Liang, X., "Tool wear, surface topography, and multi-objective optimization of cutting parameters during machining AISI 304 austenitic stainless steel flange," Metals, Vol. 9, No. 9, pp. 972, 2019.
7. Nath, C., Rahman., M., Neo K.S., "A study on the effect of tool nose radius in ultrasonic elliptical vibration cutting of tungsten carbide," J. Mater. Process. Tech. Vol. 209, No. 17, pp. 5830-5836, 2009.